

## LATERAL SPREADING MECHANISM OF A TURBULENT SPOT AND A TURBULENT WEDGE

**David Goldstein and Jeff Chu**

Department of Aerospace Engineering and Engineering Mechanics  
The University of Texas at Austin  
Austin, TX 78712  
david@ices.utexas.edu

**Garry Brown**

Department of Mechanical and Aerospace Engineering  
Princeton University  
Princeton, NJ 08544  
glb1873@msn.com

### ABSTRACT

We examine the spreading of turbulent spots and wedges into a surrounding laminar Blasius boundary layer. The spreading is not due to the lateral propagation of turbulent eddies but rather to a developing disturbance in the surrounding spanwise vorticity of the laminar boundary layer. We concentrate on the mechanisms for generating streamwise vorticity. In particular, inclined generally streamwise vortex tubes along the spot/wedge boundary tilt mean shear vortex lines either up or down. These lines subsequently tend to either lag back or lead forward. As the leading or lagging vortex lines continue to wrap around and reinforce the causative inclined tube, the lines arch up or down. The outboard portion of the resulting arch must acquire a vertical,  $\omega_y$ , component of vorticity which induces the rollup of a new inclined tube now outboard of the first. Close to the wall the arching mechanism is inhibited by the no through flow boundary condition while far from the wall the process is inhibited by the lack of sufficient mean spanwise vorticity.

### INTRODUCTION

We wish to examine two processes by which transition occurs. One is through the development and merging of turbulent spots first noted by Emmons (1951). The second process is a form of bypass transition through the formation of turbulent wedges aft of a sufficiently large surface protrusion (e.g., a dead bug on a wing). Both spot and wedge processes were observed to spread laterally linearly at half-angle of  $\sim 5\text{-}10^\circ$ . Turbulent wedges and spots have been observed for decades yet the physical mechanism that drives spreading or even why the half-angle is what it is are not fully understood. In this work, we use DNS to better understand the details of transition in both cases and if the two mechanisms are related.

Wynanski et al. (1976) and Wynanski and Zilberman (1982) studied artificially generated spots at  $Re_x$  of  $\sim 500000$  in a wind tunnel using an electrical spark for the perturbation. Like Elder (1960), they found that if the perturbation was strong enough and a spot did form it exhibited self-similar growth, independent of the initial

perturbation. Wave packets, which they believed to be TS waves, were observed near the upstream lateral edges of the spot. Wynanski et al. hypothesized that the breakdown of these wave packets led to the formation of eddies near the spanwise edges of the spot, and thus that the waves were at least partially responsible for the growth of the spots. Henningson et al. (1987) and Singer and Joslin (1994) used DNS to examine spots and observed generally good agreement with experiments but they did not identify a wave packet spreading mechanism.

A turbulent wedge, like a train of spots, is a turbulent region that diverges in the spanwise direction as it propagates downstream. Schubauer and Klebanoff (1955) observed that turbulent wedges are composed of a fully turbulent core bounded by a transitional (intermittently turbulent) region. Gad-el-Hak et al. (1981) visualized the turbulent wedge behind a short cylindrical perturbation using dye. They concluded that spanwise growth of a turbulent wedge is not like the lateral spreading of a turbulent wake but is due to a destabilization process, in which the turbulent eddies inside the wedge induce such a strong disturbance that the surrounding laminar flow is destabilized and becomes turbulent.

Zhong and Chong (2003) studied turbulent wedges using shear- and temperature-sensitive paint. They observed a spreading half-angle of about  $6.5^\circ$  for the zero pressure gradient case, which is smaller than the approximately  $10^\circ$  spreading half-angle observed by others. They attributed this to the 'spanwise overhang' of the wedge in which the turbulence does not fully extend to the wall.

Wattmuff (2004) used a vibrating ribbon to excite a sinuous instability around an artificial low-speed streak and observed a 'breakdown' of the streak into turbulence and formation of highly unsteady flow on either side of the streak centerline. The single streak 'broke down' into a turbulent wedge with a spreading half angle of about  $8^\circ$ . He postulated that the spanwise spreading of a turbulent wedge is due to a spanwise succession of streaks, where the formation of each in turn is the result of an instability introduced by the streak immediately preceding it.

We argue the following: The spot/wedge spreading mechanism is not the result of the spanwise translation of pre-existing turbulent structures nor does it arise from

vorticity diffused out of the wall. The mechanism occurs at the edge of the turbulent region, it is associated with activity at a height commensurate with the quasi-streamwise vortices which often constituting the “legs” of “hairpin” vortices close to the edge of the turbulent region, the spreading occurs in discrete steps in which new streamwise vortices are formed, and the source of vorticity forming these new vortex cores is the tilting of spanwise vorticity in the boundary layer of the surrounding laminar flow. We present justification for these statements and then describe the process by which spanwise vorticity is turned to yield the turbulent structures which form the spreading spot/wedge.

## RESULTS

The baseline wedge simulation is achieved as follows. An asymmetric cylindrical perturbation is used to trigger the formation of the turbulent wedge. The cylinder chosen has an  $Re_k$  ( $Re_k = U_\infty k / \nu$ ) of 960. The domain used for these simulations has dimensions of  $109 \delta_0$ ,  $8.7 \delta_0$ , and  $43.5 \delta_0$  in the streamwise ( $x$ ), wall-normal ( $y$ ), and spanwise ( $z$ ) directions respectively, where  $\delta_0$  is the 99% boundary layer thickness at the location of the perturbation. The computational domain has  $1152 \times 128 \times 768$  grid points in the  $x$ ,  $y$ , and  $z$  directions respectively. The origin of the turbulent wedge is at  $Re_x$  of 524,000 and the flow extends downstream to  $Re_x = 675,000$ . This corresponds to an  $Re_0$  of 480 and 566 in the laminar flow at the perturbation point and at the end of the streamwise domain, respectively.

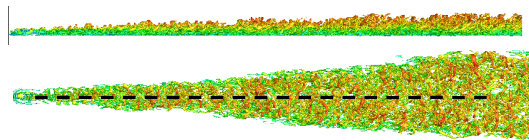


Figure 1. Turbulent wedge visualized instantaneously with iso-surface of swirling strength colored by streamwise velocity. Spreading half-angle is about  $6^\circ$ .

The result is a remarkable array of coherent structures in a turbulent wedge that exhibit many of the characteristics noted by previous researchers. Figure 1 shows side- and top-views of the turbulent wedge with iso-surfaces of swirling strength,  $\lambda_2$ , colored by streamwise velocity. The color is also a good representation of how high the iso-surface is above the wall. The swirling strength is useful for picking out vortex cores without picking up the background boundary layer shear flow. The turbulent wedge grows in width nearly linearly behind the perturbation. Arching hairpin vortices as well as quasi-streamwise structures can be observed within the wedge. The center of the wedge is dominated by a canopy of hairpin vortices that increase in size as the wedge develops downstream. The orthogonal profiles show that the turbulent wedge thickens as it spreads downstream.

In order to validate the simulation, we have compared to matched experiments done in the Texas A & M Klebanoff-Saric Quiet Flow Wind Tunnel. Briefly, we found that the structure of the surface shear stress, including individual streaks of elevated shear stress, the

asymmetry of the lateral streaks, the wedge spreading angle, and the structure of the  $U_{RMS}$  fluctuations in the fully turbulent region show close agreement between experiments and DNS.

In attempts to understand the mechanism causing a turbulent wedge to spread into the surrounding laminar flow, one possible explanation to be considered is that the turbulence is generated in the middle of the wedge and convects outward – there is a mean outward flow from the wedge centerline, for example, which could aid in such convection. One can address this possibility by asking whether the edge of the wedge can, by itself, sustain the spreading or whether the interior turbulence is necessary ‘to feed’ the edge. To answer that question, a ‘damping region’ was created to damp out the turbulence in the center of the wedge and observe its effect on the lateral propagation of the wedge. Within the damping region a body force  $\mathbf{F}(\mathbf{x}, t) = \beta \mathbf{w}(\mathbf{x}, t)$  forces spanwise velocity  $w$  toward zero, while not directly forcing the flow in the streamwise and wall-normal directions. Here,  $\beta$  is a negative constant. The damping region was also a  $6^\circ$  half angle wedge and it was introduced several roughness heights downstream. In previous studies on turbulent spots (Chu et al., 2010), we observed that damping the spanwise velocity is extremely effective in removing the turbulence.

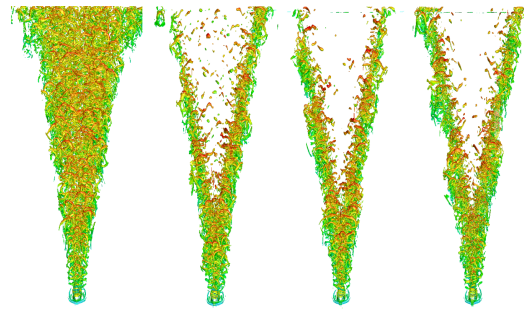


Figure 2 - Turbulent wedge under the influence of the damping region visualized as in Fig. 1. The leftmost picture is before the damping region was added; the next three pictures are at a further 0.25, 0.50, and 0.75 free-stream flow through times.

Figure 2 shows how the turbulent wedge with the damping, changes in time. The damping region is effective in removing turbulence from the core of the wedge but does not damp out turbulence along the outer edges. In the second time snapshot, it appears as though the turbulence is waning and decreasing in size, but by the third and fourth snapshot, the turbulence along the leading edge of the wedge re-intensifies. This result shows that the turbulence at the edge of the wedge is able to self-sustain without an influence from the center of the wedge. Another interesting observation is that the spreading angle appears to have changed only slightly even with the large damping region. This suggests that the cause for the characteristic spreading angle is captured along the edge of the wedge.

The observation that the spreading mechanism occurs right along the wedge boundary is surprising because if one observes animations of the flow like that in Fig. 1,

without damping, one sees the arch-like hairpin heads spread laterally and sometimes merge with one another in the center of the wedge. That is, structures identified by  $\lambda_2$  move generally downstream in the center of the wedge, but parts do appear to move laterally as well. It may be that in looking down on Fig. 1 we only see the tops of the hairpin forest which behave as described. Those arch-like vortices are reaching up and out to the edge of the region of mean shear. The active causes of the spreading mechanism however may lie much closer to the wall.

In the surrounding laminar flow there is neither  $\omega_x$  nor  $\omega_y$  vorticity. Yet along the edge of the wedge both components are present in abundance. We next examine the possibility that the spreading mechanism is linked to the diffusion out of the wall of streamwise vorticity – one of the associated mechanisms that has been proposed for the sustenance of wall bounded turbulence. In a turbulent boundary layer Suponitsky (2005) suggested that there are two proposed mechanisms of turbulence production in the near-wall region: a streak instability based mechanism and an offspring regeneration mechanism. Schoppa and Hussain (1997) proposed a streak transient growth mechanism which involves formation of a sheet of streamwise vorticity, growth of sinuous streak waviness, and streamwise vorticity sheet collapse via stretching into streamwise vortices. The offspring regeneration mechanism has been put forward by Smith and Metzler (1978), Brooke and Hanratty (1993), and Zhou et al. (1999) in which existing vortex cores create a layer of oppositely signed vorticity at the wall due to the no slip condition. Then the new vorticity leaves the wall due to the induction of its parent vortex and is stretched and intensified by the mean shear.

A key event in this latter proposed ‘offspring’ cycle in a turbulent boundary layer is the formation of secondary streamwise vorticity at the wall, which depends on the spanwise no-slip boundary condition,  $w=0$  at the solid surface. In the DNS code the no-slip conditions may be imposed independently for the spanwise and streamwise directions. This feature can be exploited by turning off the no-slip condition in the spanwise direction and observing the impact it has on the flow.

If the offspring wall cycle were a dominant mechanism in turbulence generation or spreading at the edge of the wedge, allowing spanwise slip should inhibit the formation of new streamwise vorticity hence weakening the turbulence. Conversely, if shedding streamwise vorticity off the solid wall is not an important part of the turbulence regeneration mechanism, the turbulence level should not be affected or may even increase. In simulations (not shown), the turbulent wedge for the spanwise slip case appears more vigorous and spreads at a slightly faster rate than the no-slip case. The results show that streamwise vorticity generation due to the spanwise no-slip condition is not a key factor in turbulence spreading.

Similar results were observed by Chu and Goldstein (2010) with turbulent spots in which the spanwise slip case created spots which grew more rapidly. Jimenez and Pinelli (1999) also observed similar effects in channel flow when spanwise slip was allowed. They saw increased turbulence fluctuations near the wall and a shift of the streamwise vorticity fluctuation peak closer to the wall.

Strand and Goldstein (2011) and Chu et al (2010) found that spanwise damping fins are extremely effective

in controlling the spanwise spreading of turbulent spots. Spanwise damping fins are, like the bulk damping region used above, unphysical textures that force the spanwise velocity to zero without affecting streamwise and wall-normal velocities. Figure 3 is a plan view of a turbulent spot passing over damping fins having a height of  $0.87 \delta_0$  and spacing of  $1.35 \delta_0$ . The figure shows that damping fins with height of  $0.87 \delta_0$  virtually stop spanwise spreading. The streamwise vortical structures are nearly completely ‘trapped’ between the damping fins while the heads of the hairpin vortices extend well above the fins.

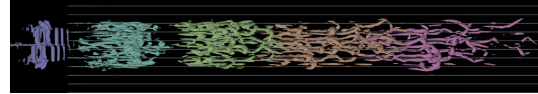


Figure 3. Time elapsed top view of a turbulent spot with damping fins of height  $0.87\delta_0$ . The turbulence does not spread in the spanwise direction. Visualized by iso-surfaces of swirling strength.

When the damping fins are about half of the maximum height of the turbulent structures, strong turbulence exists above the tops of the damping fins, yet as mentioned above, the wedge spreading is nearly completely halted. This result suggests that the spanwise spreading mechanism must be most significant near the wall where the generally streamwise vortices predominate and hairpin heads and other structures far above the plate do not induce spanwise spreading.

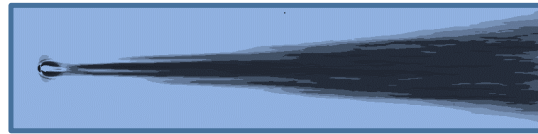


Figure 4. Time-averaged surface shear stress contours below a turbulent wedge.

As seen in Fig. 4, the spreading process appears to occur, in the mean, in discrete increments. To clarify the mechanism for these jumps, an average velocity field in the turbulent wedge is obtained by taking the time average over approximately five free-stream flow-through times. Figure 5 shows the resulting iso-surface of streamwise velocity colored by distance from the wall. This figure shows some distinct structures along the edges of the turbulent wedge that are low-speed streaks that remain stationary in the mean. There are essentially stationary collar vortices coming from the roughness element which are also seen for smaller subcritical discrete roughness elements (Doolittle et al, 2014). The collar vortices ‘pin’ the initial streamwise vortices. New vortices form outboard of that first set of pinned vortices, and so on. This could also explain why the structures are more distinct near the roughness element while they become more washed out further away from the pinning primary collar vortex: upstream random fluctuation would produce cumulative smearing of the time averaged structures further outboard.

This discrete development of a streak suggests that the spanwise growth of the wedge is the result of the formation of a spanwise succession of streaks, where the formation of each, in turn, is the result of an instability introduced by the vorticity field preceding it upstream.

These discrete streaks are approximately 120 wall units apart, calculated using the average velocity gradient underneath the wedge (blue regions in Figure 5). Also displayed are  $\lambda_2$  iso-surfaces on top of the mean streamwise velocity iso-surface. One can observe how the instantaneous turbulent structures align themselves over the rippled mean velocity sheet that marks the discrete streaks. Note that on the outboard side of the rippled mean velocity iso-surface the quasi-streamwise  $\lambda_2$  structures tilt both forward and backward. That is, the structures there are not only the ‘legs’ of hairpin vortices.

In a sense the roughness element not only pins the streamwise structures that manifest themselves as the discrete streaks but it also pins the origin of the wedge in the streamwise direction. A turbulent spot, however, is generally created by an impulsive or short-lived disturbance and once the disturbance is over there is nothing to pin the upstream side and it withers from behind even as it grows and spreads downstream. The fixed roughness element is sufficient to cause and sustain immediate bypass transition that then spreads laterally.

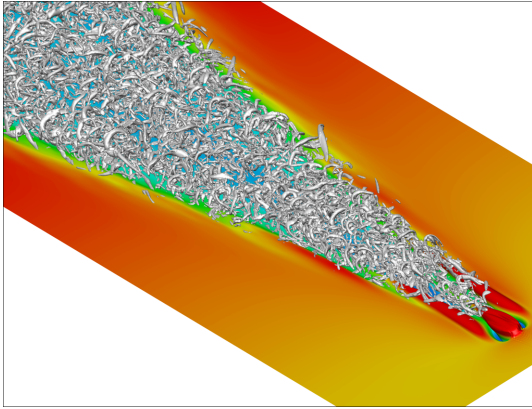


Figure 5. Time averaged low speed streaks visualized by sheet-like iso-surface of  $U/U_{inf} = 0.25$  colored by distance from the wall. The discrete structures are low-speed streaks with approximately 120 wall units lateral spacing. Instantaneous  $\lambda_2$  iso-surface structures are superimposed on top of velocity iso-surface sheet.

What is the source of the vorticity forming the growing outer edge of the wedge? In Fig. 6 we plot  $\lambda_2$  iso-surfaces above low level iso-surfaces of  $\omega_x$ . One observes a remarkable pattern of alternating tilted ‘pancakes’ of streamwise vorticity perturbations extending well outboard of the sensible turbulent structures. The cloverleaf pattern of  $\omega_x$  iso-surfaces situated immediately about the roughness element is static and is caused by the steady lateral displacement of the near-wall flow about the element (Doolittle et al, 2014). Starting several roughness heights downstream, however, the alternating tilted ‘pancakes’ of  $\omega_x$  perturbations are moving downstream. Similar structures are found in turbulent spots (Chu and Goldstein, 2010).

Determining how new vortices are formed is key to understanding how the wedges spread and the ‘pancakes’ of  $\omega_x$  perturbations are clues. Since newly generated vortices are predominantly streamwise, the essential dynamics of vortex formation are likely those of  $\omega_x$ , whose inviscid evolution is governed by Equation (1):

$$\frac{\partial \omega_x}{\partial t} = -u \frac{\partial \omega_x}{\partial x} - v \frac{\partial \omega_x}{\partial y} - w \frac{\partial \omega_x}{\partial z} + \omega_x \frac{\partial u}{\partial x} + \frac{\partial v}{\partial x} \frac{\partial u}{\partial z} - \frac{\partial w}{\partial x} \frac{\partial u}{\partial y}$$

(1)      Self Induction      Stretching      Tilting

If the contours of the three terms that determine the local change in streamwise vorticity, i.e. self-induction, stretching and tilting, we find tilting is the largest term at the wedge edge where new vortices are forming. The tilting term is associated with tilted pancake structures outboard of the  $\lambda_2$  turbulent structures. Not surprisingly, the second half of the tilting term,  $-(\partial w / \partial x)(\partial u / \partial y)$ , dominates the tilting term due to the strong mean velocity gradient  $\partial u / \partial y$  and it is largely responsible for the existence of the  $\omega_x$  ‘pancakes’. The  $(\partial v / \partial x)(\partial u / \partial z)$  component does not contribute appreciably.

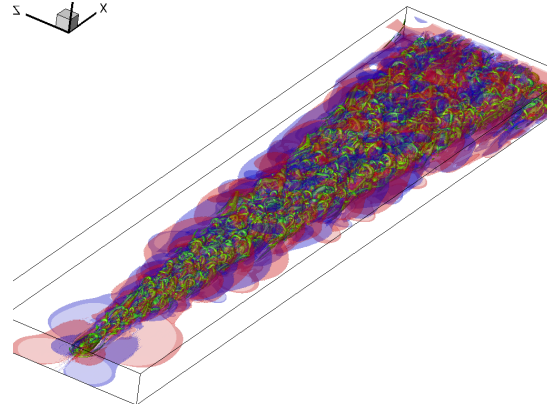


Figure 6. Turbulent wedge visualized with  $\lambda_2$  iso-surfaces and translucent  $\pm \omega_x$  iso-surfaces. Note the alternating tilted layered ‘pancake’ structure.

A key question that follows is, what part of the turbulent wedge structure drives the tilting of spanwise vorticity into the streamwise direction due to  $(\partial w / \partial x)(\partial u / \partial y)$ ? The mean shear  $\partial u / \partial y$  term is positive and relatively large over a substantial part of the laminar boundary layer. To understand the source of  $\partial w / \partial x$ , one must look at the velocity field induced by the vortical structures at the edge of the wedge. At the height of the ‘pancakes’, the most outboard vortical structures at the edge of the wedge are inclined vortex tubes. Figure 7 shows a contour slice of the spanwise velocity,  $w$ , around a tilted vortical structure visualized as one grey iso-surface of  $\lambda_2$  which in this case appears to be a ‘leg’ and part of a ‘head’ of a hairpin vortex. The vortical structure clearly induces an outboard velocity above (yellow region) and an inboard velocity (blue) below. Thus the structure induces a spanwise velocity change from positive to negative. Fig. 7(b) shows the corresponding iso-surface of  $\partial w / \partial x$  near this structure.

The layered red-blue-red  $\partial w / \partial x$  structures stem from the combination of the tilt of the vortical structure and the induced spanwise velocity. A simplified situation is shown in Fig. 8 to illustrate how  $\partial w / \partial x$  can arise due to the vortical motion of the tilted structure and how there would be a positive  $\partial w / \partial x$  iso-surface both upstream

and downstream of the vortical structure and negative  $\partial w / \partial x$  right at the structure. One isolated tilted vortical tube can generate three tilted pancake layers that alternate in sign. This agrees with our previous observations of many tilted pancake layers that seem to move at the same speed as the tilted vortical structures.

We suggest a mechanism by which an existing vortical structure – an inclined, generally streamwise-aligned vortex leg – can generate new streamwise vorticity in the adjacent region of laminar, uniform background shear,  $\partial u / \partial y$ . This inclined vortex tube tilts the prevailing spanwise vorticity into the streamwise direction in pancake-shaped regions, which can be viewed as associated either with the  $\partial w / \partial x$  term or as regions of a perturbation of  $\pm \omega_x$  vorticity, just outboard of the causative inclined vortex tubes. These observations agree with our non-physical experiments in which we found that the spanwise no-slip condition at the bottom wall is not important and spreading seems to occur *near* the wall, but *not directly* at the wall.

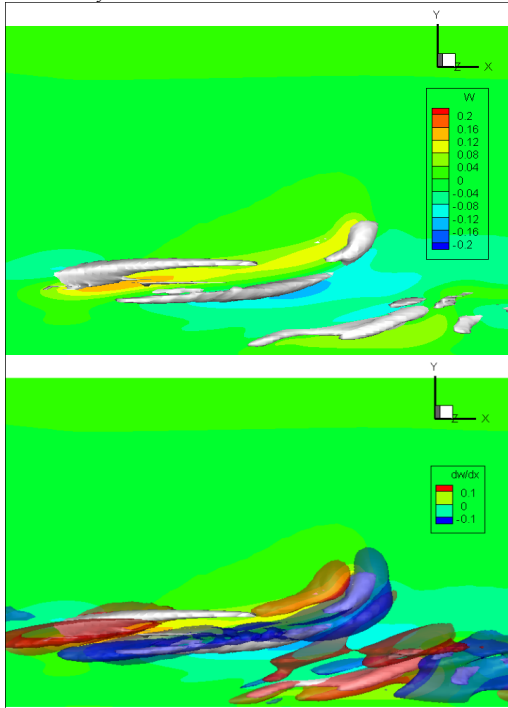


Figure 7. (a) Spanwise velocity contour (slice) around a grey iso-surface of a vortical leg. (b) Same as (a) except with additional  $\partial w / \partial x$  iso-surfaces. Notice the formation of red-blue-red layers associated with the tilted grey vortical structure.

The connection is now made between the creation of  $\omega_x$  vorticity via tilting, and its accumulation into new inclined tubes of vorticity, which can continue the process and cause the lateral spreading of the turbulence. Fig. 9 shows vortical structures accumulating the tilted spanwise vorticity. Existing legs can turn spanwise vortex lines forward and backwards and some vortex lines are wrapped into a new vortex. Existing vortical structures are identified by  $\lambda_2$  now colored by streamwise vorticity. Also drawn are vortex lines similarly colored by  $\omega_x$ . In the

laminar flow spanwise vortex lines originate at the edge of the domain at a height midway between the top of the turbulent wedge and the wall. As they are propagated inward, some lift upward and then, finding themselves in higher speed flow, tilt forward. These lines turn red. Those lines which tilt downward, lag back and turn blue as vorticity develops a negative  $\omega_x$  component.

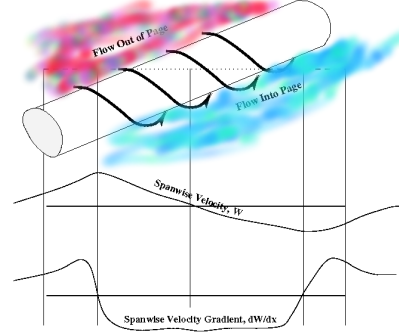


Figure 8. Schematic view of regions of positive and negative spanwise velocity around an inclined streamwise vortex having positive  $\omega_x$ .

A common feature found along the edge of the wedge is that the lifting and tilting produces an arching up of vortex lines. Three or four such regions are seen in Fig. 9. If an inclined tube is red (has  $+\omega_x$  vorticity) then just upstream and to the outboard side of the tube there is a region of positive  $\partial w / \partial x$  as indicated schematically in Fig. 8. Hence,  $(\partial w / \partial x)(\partial u / \partial y)$  there is positive and that produces negative  $\omega_x$  vorticity through tilting, as in Eq. 1. This is also the region where Biot-Savart induction is causing the flow to dip down and spanwise vortex lines which dip down begin to lag the local flow and turn into negative  $\omega_x$  vorticity. Conversely, the blue, negative,  $\omega_x$  vorticity tubes on the starboard side of the wedge seen in Fig. 9 are creating negative  $\partial w / \partial x$  ahead and outboard leading to the generation of positive  $\omega_x$  vorticity further outboard. The other way to view the situation is that the blue, negative,  $\omega_x$  vorticity tubes are causing the spanwise vortex lines to arch up and on the outboard side of the arch the resulting positive  $\omega_x$  vorticity begins to roll up into a new positive (red) vortex tube. We expect there to be a bias toward blue, negative,  $\omega_x$  vorticity tubes being more effective in propagating the turbulence outboard because they *lift up* the spanwise vortex lines – the vortex lines are unimpeded in their upward motion. A red or positive  $\omega_x$  vorticity tube, however, must push the vortex lines down and the wall impedes this.

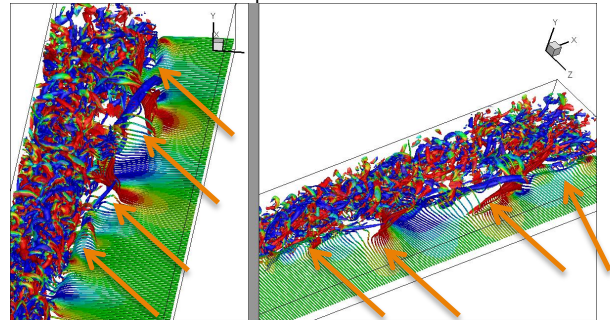


Figure 9.  $\lambda_2$  vortex tubes and vortex lines colored by  $\omega_x$  vorticity. Two views are shown of the starboard side of

the turbulent wedge. Arrows highlight arching vortex lines.

## SUMMARY

We make the following observations:

1. The turbulent regions obviously contain substantial streamwise vorticity,  $\omega_x$ . For the lateral spreading, streamwise vorticity is not predominantly drawn out of the wall from the no-slip condition but it develops from the tilting and stretching of the background spanwise vorticity of the laminar boundary layer.
2. The tilting mechanism occurs well above the wall but within the laminar boundary layer and well below the tops, or heads, of the hairpin-like structures in the turbulent region.
3. In a turbulent wedge, the initial lateral spreading appears to occur in discrete steps.
4. The spreading mechanism is confined to the periphery of the spot or wedge – it is not driven by turbulence in the center of the spot or wedge.
5. There are periodic disturbances seen as tilted ‘pancakes’ of  $\omega_x$  along the boundary of a spot or wedge which are a signature of the vorticity tilting process turning  $\omega_z$  into  $\omega_y$  and  $\omega_x$ .
6. The source of these tilted ‘pancakes’ of perturbation streamwise vorticity are ‘tubes of vorticity at the edge of the turbulent wedge. Through the Biot-Savart relation these tubes lift up and push down vortex lines and the primary velocity gradient tilts the vortex lines to add to the streamwise vorticity and give rise to a concentration of streamwise vorticity. This begins a new vortex tube whose local circulation then self-amplifies through the further wrapping up of vortex lines.

It seems that the spreading mechanism for spots and wedges is essentially the same for the following reasons. Inclined vortex tubes along the periphery tilt spanwise vortex lines in the laminar boundary layer either up or down. On the starboard side of the wedge or spot those vortex lines tilted down tend to lag back producing  $-\omega_x$  vorticity (blue) while those tilted upward tend to lean forward and produce  $+\omega_x$  (red). Since the causative vortex is inclined, so are the resulting red and blue  $\omega_x$  ‘pancake-regions’. As the leading or lagging vortex lines continue to wrap around and reinforce the causative inclined tube, the lines arch up or down. The outboard portion of the resulting arch must acquire a vertical,  $\omega_y$ , component of vorticity which induces the rollup of a new inclined tube now outboard of the first. Close to the wall the arching mechanism is inhibited by the no through flow boundary condition while far from the wall the process is inhibited by the lack of sufficient mean spanwise vorticity. Finally, regions of creation of new streamwise vorticity on the boundary are associated with the  $\partial w / \partial x$  term in the vorticity tilting portion of the equation for the local development (rate of change) of streamwise vorticity.

## ACKNOWLEDGEMENTS

This work was supported in part by AFOSR grants FA 9550-08-1-0453 and FA 9550-11-1-0203.

## REFERENCES

- Brooke, J.W. and Haratty, T.J., “Origin of Turbulence-producing Eddies in a Channel Flow,” *Phys. Fluids*, Vol. 5, 1993, pp.1011.
- Chu, J., Strand, J., and Goldstein, D. “Investigation of turbulent spot spreading mechanism.” AIAA Paper, Orlando, 2010.
- Doolittle, C., Drews, S. and Goldstein, D. 2014. “Near-field flow structures and transient growth due to subcritical surface roughness,” *Phys. of Fluids*. **26**, 123106.
- J.W. Elder, 1960, “An Experimental Investigation of Turbulent Spots and Breakdown to Turbulence,” *JFM*, **9**, pp.235-246.
- Emmons, H. W. , “The Laminar-Turbulent Transition in a Boundary Layer - Part I,” *J. Aeronautical. Sciences*, Vol. 18, No. 7, July 1951, pp. 490-498.
- M. Gad-el-hak, et al., 1981, “On the Growth of Turbulent Region in Laminar Boundary Layers,” *JFM*, Vol. **110**, 1981. pp. 73-95
- D. Henningson, P. Spalart, and J. Kim, 1987, “Numerical Simulations of Turbulent Spots in Plane Poiseuille and Boundary Layer Flow,” *Physics of Fluids*, Vol. 30, No. 10, pp. 2914-2917.
- Jimenez, J., and Pinelli, A., “The Autonomous Cycle of Near-wall Turbulence” *JFM*, Vol. 389, 1999, pp.335-359
- G.B. Schubauer and P.S. Klebanoff, 1955, *Contributions on the Mechanics of Boundary-Layer Transition*, NACA N-3489
- P.J. Schmid and D. S. Henningson, 2001. *Stability and transition in shear flows*. New York: Springer.
- Schoppa, W. and Hussain, F., “Genesis and Dynamics of Coherent Structures in Near-wall Turbulence: A New Look,” *Self-Sustaining Mechanism of Wall Turbulence*, edited by Panton, R. L., Advances in Fluid Mechanics, Vol. 15, (1997) pp. 385-422.
- Singer, B., and Joslin, R. “Metamorphosis of a Hairpin Vortex into a Young Turbulent Spot,” *Physics of Fluids*, Vol.6, No. 11, Nov. 1994, pp.3724-3736.
- Smith, C.R. and Metzler, S.P., “The Characteristics of Low-speed Streaks in the Near-wall Region of a Turbulent Boundary Layer,” *JFM*, Vol. 129, 1978, pp.27.
- J. Strand, D. Goldstein, 2011 “DNS of Surface Textures to Constrain the Growth of Turbulent Spots,” *JFM*, **668**, p. 267-292, DOI: 10.1017/S0022112010005033.
- Suponitsky, V., Cohen, J., and Bar-Yoseph, P., “The Generation of Streaks and Hairpin Vortices from a Localized Vortex Disturbance Embedded in Unbounded Uniform Shear Flow,” *JFM*, Vol. 535, 2005, pp.65-100.
- J.H. Watmuff, “Evolution of a Turbulent Wedge from a Streamwise Streak,” 15th Australasian Fluid Mechanics Conference, Sydney, Australia. December 2004
- J. Wignanski, M. Sokolov and D. Friedman, 1976, “On a turbulent ‘spot’ in a laminar boundary layer,” *JFM*, **78**, 785-819.
- Wignanski, I. J., and Zilberman, M., “On the Spreading of a Turbulent Spot in the Absence of a Pressure Gradient,” *JFM*, Vol. 123, 1982, pp.69-90.
- S. Zhong, T. Chong, 2003, “A Comparison of Spreading Angles of Turbulent Wedges in Velocity and Thermal Boundary Layers,” *J. of Fluid Eng.*, Vol. **125**, pp.267-75.
- Zhou, J., Adrian, R., Balachandar, S. and Kendall, T., “Mechanism for Generating Coherent Packets of Hairpin Vortices in Channel Flow” *JFM*, Vol. 387, 1999, pp.35.